Applied Geochemistry 98 (2018) 36–44

Contents lists available at ScienceDirect

Applied Geochemistry

journal homepage: www.elsevier.com/locate/apgeochem

Comparison between cesium and sodium retention on calcium silicate hydrate (C—S—H) phases

Tiziana Missana*, Miguel García-Gutiérrez, Manuel Mingarro, Ursula Alonso

CIEMAT, Physical Chemistry of Actinides and Fission Products Unit, Department of Environment, Avenida Complutense 40, 28040 Madrid, Spain

ARTICLE INFO

Keywords:
Cesium
Radioactive waste
Calcium silicate hydrate
Surface complexation modelling

ABSTRACT

Batch sorption experiments and sorption modelling were combined to analyse the mechanisms of Cs and Na retention on calcium silicate hydrate phases, C—S—H, and to identify similitudes/differences between the two elements.

The role played by the C—S—H's Ca/Si ratio and the tracer concentration on alkali ions retention was experimentally analysed. For both elements, sorption decreased when the Ca/Si ratio increased, but only in the case of Cs sorption was clearly not linear.

Distribution coefficients (K_d) for Cs were higher than those of Na at trace concentration and low Ca/Si ratio but at high alkali concentrations, K_d values for Cs and Na were always comparable. This was a first indication that low-density but high selective sorption sites exist on the C—S—H surface, accessible for Cs and not for Na.

Electrophoretic measurements were carried out to evaluate the variation of the C—S—H surface charge (ζ-potential) upon alkali addition and to support modelling studies. Under similar experimental conditions, the change produced by Cs or Na additions on the ζ-potential of the gels was always similar.

Different sorption models were proposed to fit the experimental data, based on the adsorption data, on the variation of C—S—H surface potential upon Cs/Na sorption and on previous tests showing the competitive effects of Na and Cs on Ba uptake. Their adequacy will be discussed as well as the differences/similitudes of sorption behaviour for both elements.

1. Introduction

Cement-based materials are used in radioactive waste repositories because, for their physical and chemical properties, they are adequate for the immobilisation of toxic wastes (Atkins and Glasser, 1992; Chen et al., 2009; Ochs et al., 2016). Calcium silicate hydrate (C—S—H) gels are the main cement hydration products; they are amorphous or poorly crystalized materials with elevated surface area ($> 100\,m^2\,g^{-1}$) and variable chemical composition ($xCaO{\cdot}SiO_2{\cdot}yH_2O$), which are expected to control cation retention in cement.

The Ca/Si ratio of C—S—H gels is responsible of the different physical-chemical characteristics of the cement (Chen et al., 2004) during different aging stages, and consequently it also affects its overall sorption capability.

Cesium (^{137}Cs) is a critical radionuclide (RN) in the frame of radioactive waste repositories because it exists in aqueous solution mainly as the cation Cs^+ presenting very high solubility. Other alkalis, such as sodium and potassium are of special importance in the cementitious environments because their concentration is often elevated in cement pore-water; furthermore, their presence was observed to decrease cation retention on C—S—H phases (Tits et al., 2006; Lothenbach and Nonat, 2015; Missana et al., 2017).

Ochs et al. (2016) reviewed sorption data on cementitious materials of several RNs, providing sorption coefficients databases and linking the results to various stages of cement degradation. In the case of Cs, a relatively high dispersion of distribution coefficients (K_d) was reported, but K_d values were not especially high ($< 1{\cdot}10^3\,mL\,g^{-1}$). It was observed that Cs is mainly retained in C—S—H phases and that its sorption tends to increase as cement degrades; indicating that dissolved Na, K and Ca in porewater may compete with Cs for sorption sites and suggesting that a possible sorption mechanism for Cs in hardened cement pastes (HCP) is ionic exchange in the C—S—H phases. In many papers, a clear dependence of alkali sorption on Ca/Si ratio was reported (Hong and Glasser, 1999; Pointeau, 2000; Viallis-Terrisse et al., 2002; Lothenbach and Nonat, 2015; Henocq, 2017) which indicates that the presence of high quantity of Ca in solution (high Ca/Si) inhibits the cation uptake.

Nevertheless, Viallis-Terrisse et al. (2002) suggested the existence of

* Corresponding author.
E-mail address: tiziana.missana@ciemat.es (T. Missana).

https://doi.org/10.1016/j.apgeochem.2018.09.007
Received 5 February 2018; Received in revised form 31 May 2018; Accepted 5 September 2018
Available online 06 September 2018
0883-2927/

specific interactions of Cs with the surface of C−S−H and the formation of inner-sphere complexes with silanol sites, not observed for Na, which was considered an "indifferent" ion for the gels (Viallis et al., 1999). They suggested that Cs and Na behave different due to their different hydration energies (smaller for Cs than Na), which induce different degrees of interaction with the surface. Iwaida et al. (2002) observed that Cs sorption (at least at high concentration) in C−S−H caused the fragmentation of the torbermorite-type structure, not observed upon the interactions with Na.

Evans (2008) also reviewed sorption studies of different RNs on cementitious materials; for alkalis he reported that their sorption on C−S−H increases inversely to the Stokes radius of the hydrated ions, and that sorption might be electrostatic on a negatively charged C−S−H sites (even if the mechanisms for positively charged C−S−H are not mentioned). Ionic exchange with Ca, is cited as possible mechanism for Na sorption.

Bach et al. (2013) studied the adsorption behaviour of K and Na and suggested that the first may enter and be retained in the C−S−H *interlayers* whereas Na cannot. Instead, Stade (1989), reported nearly equal binding capacities for Na and K in C−S−H, similarly to the results obtained by Hong and Glasser (1999).

Thus, despite the relatively large number of studies on alkalis retention in cementitious materials, a clear picture of their sorption mechanisms does not exist. In particular, attempts to model Cs or Na retention on cementitious materials by thermodynamic (mechanistic) models are relatively scarce. Given the C−S−H structure and properties, and as reported in the literature, different sorption mechanisms for cations might be postulated, from ion-exchange and/or surface complexation, as well as *"electrostatic"* interactions. Sugiyama (2008) employed an ion-exchange model to simulate the effects of NaCl on the alteration of C−S−H, assuming Na−Ca exchange as the responsible of Ca release in the presence of the salt.

Heat et al. (1996) modelled single K_ds of Cs, obtained at different Ca/Si ratios using a double layer approximation and assuming surface complexation on silanol groups.

Ochs et al. (2006) studied Cs sorption on cements as a function of the degradation state and modelled the experimental data with a surface complexation model, formerly developed by Pointeau (2000), which included surface complexation on weak and strong silanol sites, with the density of strong silanol sites depending on the Ca/Si ratio.

Henocq (2017) proposed a model for Na in cement-based materials integrating retention and ζ-potential data, as well as solubility data, pointing out the necessity of coupling independent data for a consistent determination of model parameters. The author proposed a triple layer surface complexation model, using the CD-MUSIC method.

Missana et al. (2017) determined the complexation constants and selectivity coefficients for Na, Cs and K assuming a three-sites model (SWE, with strong (S) and weak (W) complexation sites and ion exchange site (E)), which were indirectly determined through the analysis of the competence effects of the alkali ions on Ba adsorption (on a C−S−H with Ca/Si = 0.8). Their presence decreased Ba uptake in the following order Na < Cs < K. The value of $\log K_d$ for Ba, that was 3.8 in the absence of alkalis, decreased to approx. 3, 2.9 and 2.7 in the presence of $5{\cdot}10^{-2}$ M of Na, Cs and K respectively, clearly indicating competence of the three ions with Ba and a different selectivity for the C−S−H surface, but not necessarily a different sorption behaviour.

The objectives of the present work are: 1) to analyse the sorption of Cs and Na on different C−S−H phases evaluating their similitudes/differences; 2) to validate the description of the C−S−H surface properties proposed by Missana et al. (2017) and to verify the adequacy of their three-sites model (SWE) for reproducing Cs and Na sorption data under a wider range of experimental conditions and 3) to appraise the possibility of using simplified models to fit the sorption behaviour of these elements.

To accomplish these aims, batch sorption experiments were carried out to evaluate the effect of Ca/Si ratio and of alkalis concentration on their adsorption; parallel studies were made to evaluate the response of the C−S−H surface charge (ζ-potential) to alkali additions. The proposed sorption models should be able to reproduce not only the Cs and Na sorption behaviour, but also the variation of C−S−H surface potential before and after alkalis uptake.

Previous data of the competitive effects of Na and Cs on Ba adsorption (Missana et al., 2017) were also accounted for, as an additional constraint because the determination of model parameters sometimes resulted to be ill-defined.

2. Materials and methods

2.1. C−S−H gels preparation and characterisation

Four C−S−H phases with different CaO/SiO_2 (Ca/Si) molar ratios were prepared; the target Ca/Si ratios were: 0.8, 1, 1.2 and 1.6. They will be referred to as: C−S−H (0.8); C−S−H (1); C−S−H (1.2) and C−S−H (1.6). The method used for producing the phases was the *"direct method"* already described elsewhere (Pointeau, 2000).

The gels preparation was carried out in an anoxic glove box, under N_2 atmosphere (O_2 < 1 ppm). For their synthesis CaO (Alfa Aesar 99,95% purity) and SiO_2 (Aldrich 99,8% purity) were used. Both solids were weighted to obtain the requested molar Ca/Si ratios and a solid to liquid ratio of 10 g L^{-1}, afterwards they were mixed to 1L deionised water previously boiled and bubbled with N_2 to minimize the CO_2 content. Deionised water was obtained with a Siemens Ultra Clear water purification system.

The suspensions were prepared in HDPE dark bottles and maintained under stirring to obtain a homogeneous product. Conductivity and pH were periodically measured until the steady-state was reached (approximately 10–15 days) indicating the completion of the synthesis process.

Measurements of pH (± 0.10) were made using a Mettler Toledo (S220) pH-meter with a solid polymeric electrode (Xerolyt) or a Crison pH-ion meter (GLP225) with a combined glass pH electrode (Metrohm). Electrodes calibration was made with buffer solutions at pH 2.00, 4.00, 7.00, and 10.00. Conductivity measurements were carried out with a Crison EC Meter Basic 30^+. The final pH and conductivity of the gel suspensions as well as Ca and Si in solution are specific for each Ca/Si ratio and summarised in Table 1.

Sorption experiments were carried out directly with these suspensions (10 g L^{-1}). Upon the formation of the C−S−H phases, an aliquot of 250 mL of the suspensions was filtered by 0.1 μm. Part of the supernatant (50 mL) was used for Ca and Si quantification, and the other fraction was stored for its use for sample dilutions. Ca and Si in the supernatant were measured by ICP-OES with a VARIAN 735 ES spectrometer.

The BET surface area of the samples was measured by N_2 adsorption: the mean N_2-BET value measured for C−S−H phases with Ca/Si 0.8, 1 and 1.2 was 144 ± 40 m^2/g. This BET value is in good agreement with that reported by other authors (Tits et al., 2006b, 148 m^2/g).

Nevertheless, the value measured in the C−S−H (1.6) was approximately halved (73 m^2/g) and this can be explained by the possible precipitation of portlandite during the preparation of the phases.

Atomic force microscopy (AFM), in tapping mode, was used to analyse their microstructure with a Nanoscope IIIa apparatus (Digital

Table 1
Chemical analyses of the solid or supernatant of the C−S−H phases.

Sample	pH	Conductivity (μS·cm^{-1})	Ca (mg·L^{-1})	Si (mg·L^{-1})
C−S−H (0.8)	10.38	201	44	75
C−S−H (1.0)	11.41	926	82	4
C−S−H (1.2)	12.19	2140	204	1.5
C−S−H (1.6)	12.37	6240	600	0.2

Instruments). AFM samples were prepared depositing a drop of the suspensions onto a freshly cleaved mica substrate (after Poly-L-Lysine coating) and left drying in the anoxic chamber under N_2 atmosphere overnight. AFM image analysis was carried out with the WSXM 4.0 software (Horcas et al., 2007).

2.2. C–S–H gels surface charge characterisation

The ζ-potential of the C–S–H phases (initial and upon alkali addition) was measured by means of the laser Doppler electrophoresis technique using a Malvern Zetamaster apparatus equipped with a 5-mW He–Ne laser (λ = 633 nm, scattering angle 90°). The ζ-potential was calculated from the measured electrophoretic mobility using the Smoluchowski equation (Hunter, 1991).

The samples for electrokinetic measurements were diluted to 1 g/L with the supernatant in equilibrium with the solid, obtained by filtering the initial suspension, as explained in Paragraph 2.1, because measurements with high solid/liquid ratio did not give reliable results.

The variation of the surface potential upon CsCl or NaCl addition (from $2{\cdot}10^{-3}$ to $5{\cdot}10^{-2}$ M) to diluted C–S–H, was measured after three days of contact time to ensure alkali sorption.

Particle size was measured with a ZetaSizer Nano ZS (Malvern) (He–Ne laser, λ = 633 nm, scattering angle 173°). In all the C–S–H phases, the suspended particles were observed to form big aggregates with size larger than 1 μm.

2.3. Radionuclide and counting techniques

The radionuclides used for this study were ^{137}Cs and ^{22}Na. Cesium was supplied by Isotope Products as CsCl in 0.1 HCl. The half-life of ^{137}Cs is 30.2 years. This radionuclide decays by beta emission to ^{137m}Ba, responsible of the emission of gamma rays (662 keV). Sodium was supplied by Perkin Elmer as NaCl in water. The half-life of ^{22}Na is 2.6 years, it decays by beta emission and gamma rays of 1275 keV are present. Thus, the activity in solution of both RNs was measured by γ-counting with a NaI detector (Packard Autogamma COBRA II). The uncertainty for the counting procedure is less than 2%.

2.4. Sorption tests

Sorption data were obtained using a batch sorption technique. Experiments with the different C–S–H phases (10 g L^{-1}) were carried out in anoxic glove box under N_2 atmosphere and at room temperature. The effect of RN concentration was analysed, as well as the kinetics of the sorption process. Sorption kinetics was investigated for Cs, on the C–S–H (0.8) and C–S–H (1.2), to determine the time required for the attainment of the sorption equilibrium. The suspensions (10 mL), were introduced in centrifuge tubes, traced with the radionuclide ([Cs] = $1.4{\cdot}10^{-9}$ M) and maintained in continuous stirring during the selected contact time (from 1 to 91 days).

Sorption isotherms of Cs were carried out with four C–S–H phases (Ca/Si = 0.8, 1, 1.2 and 1.6) whereas only two phases (Ca/Si = 0.8 and 1.2) were used for Na sorption isotherms. In the isotherms, the radionuclide concentration varied approximately from $1{\cdot}10^{-9}$ M to $5{\cdot}10^{-2}$ M. The highest concentrations were achieved adding stable Cs or Na in the form of CsCl or NaCl (high purity chemicals). The contact time for the sorption isotherms was fixed to 15 days.

After the desired contact time, the solid and liquid phases were separated by centrifuging (25000 g, 30 min), with a JOUAN MR23i centrifuge. After the solid separation, three aliquots of the supernatant were extracted from each tube for the analysis of the final Cs or Na activity. The rest of the solution was used to check the final pH.

The degree of sorption was represented by the distribution coefficient K_d (mL·g^{-1}), defined as the ratio of the mass (activity) of the element per unit mass of the solid to the mass (activity) per unit volume of the solution. It is calculated with this formula:

$$K_d = \frac{C_{in} - C_{fin}}{C_{fin}} \cdot \frac{V}{m} \qquad \text{E.1}$$

C_{in} and C_{fin} are the initial and final concentrations of tracer in the liquid phase (Bq·mL^{-1}), m the mass of the gel (g) and V the volume of the liquid (mL).

Sorption onto vials and ultracentrifuge tubes was checked after sorption experiments; it was always lower than 2% and therefore it was not accounted for in K_d calculations.

2.5. Sorption modelling

Sorption models will be tested considering Cs and Na sorption isotherm data, the variation of the ζ-potential increasing the concentration of alkalis and additional data on competition effects of Cs/Na on Ba adsorption.

The basis for the description of the C–S–H surface properties used for sorption modelling have been previously described in Missana et al. (2017), that proposed the existence of three different sites on the C–S–H surface that can be active in cation adsorption. Basically, in the model, the existence of two types of silanol sites (SiOH) with different selectivity for cations was postulated (strong, S, and weak, W) as well as the existence of ion exchange sites, E, with Ca (X_2Ca). The density of weak and strong silanol sites is 13 and $3.5{\cdot}10^{-3}$ μmol m^{-2}, respectively, and the density of exchange sites 2 μmol m^{-2}.

For simplicity, all the models are named, according to the used sites, therefore the 3-sites model (Missana et al., 2017) is SWE.

Sorption on silanol sites was described in terms of surface complexation reactions, considering a classical diffuse double layer (DDL) model approach (Huang and Stumm, 1973; Dzombak and Morel, 1990).

In the DDL model, it is supposed that sum of the charge at the solid surface, σ_0, and the charge in the diffuse layer σ is null ($\sigma + \sigma_0 = 0$); then this approximation neglects the compact part of the double layer and the diffuse potential, Ψ, is equivalent to the surface potential Ψ_0. According to the Gouy-Chapman description; the relationship between the potential, ψ, and charge density, σ, in DDL is given (for a symmetric electrolyte) by:

$$\sigma = -0.1174\sqrt{I}\sinh\left(\frac{ze\Psi}{2kT}\right) \qquad \text{E.2}$$

In this expression, σ is expressed in C/m^2; Ψ in V; k is the Boltzmann constant, T the absolute temperature, e the electron charge, z the electrolyte valence and I the ionic strength of the solution in mol/L.

The direct measurement of the surface potential is not possible, therefore the concept of ζ-potential (or electrophoretic potential) is often used for modelling purposes. The ζ-potential is the potential generated by the surface charge at the location of the "*slipping plane*", which limits the layer of fluid adhered to the particle and moving with it. The exact position of this plane cannot be determined, but it can be assumed that ζ-potential is equal or very close to the diffuse layer potential (Hunter, 1992; Delgado et al., 2007). This assumption will be used for modelling purpose and the experimental ζ-potential will be compared with the calculated Ψ.

As previously mentioned, cation adsorption in the C–S–H phases can take place on the weak or strong silanol sites, SiOH which, under alkaline conditions, are deprotonated according to the following reaction:

$$SiOH \underset{K-}{\Leftrightarrow} SiO^- + H^+ \qquad \text{(E.3)}$$

Being K− the intrinsic equilibrium acidity constants. The mass law equations corresponding to the reaction E.3 is:

$$K_- = \frac{(SiO^-)\{H^+\}}{(SiOH)} exp\left(\frac{-F\Psi}{RT}\right) \qquad \text{(E.3a)}$$

where {} represents the ion activity and () the ion concentrations. Ψ

represents the surface potential; R the molar gas constant; T the absolute temperature (K); and F the Faraday constant. Since the activity coefficients for all the surface species are assumed to be equal, the activities of these species can be substituted by their concentrations. The exponential represents the columbic term that accounts for the electrostatic effects (Dzombak and Morel, 1990).

In the case of cation surface complexation, reactions of this type can be assumed:

$$SiO^- + M^{z+} \underset{K_C}{\Leftrightarrow} SiOM^{z-1} + H^+ \quad \text{(E.4)}$$

$$K_C = \frac{(SiOM^{z-1})\{H^+\}}{(SiO^-)} exp\left(\frac{-F\Psi}{RT}\right) \quad \text{(E.4b)}$$

Of special importance the reaction with Ca, which is the ion determining the potential (IDP) of C–S–H:

$$SiO^- + Ca^{2+} \underset{K_{Ca}}{\Leftrightarrow} SiOCa^+ \quad \text{(E.4c)}$$

For what concerns cation exchange, it is assumed that initially exchange sites are occupied by Ca (X_2Ca). In the case of exchange with a monovalent ion (M^+) the reaction can be written as:

$$X_2Ca + 2M^+ \leftrightarrow 2XM + Ca^{2+} \quad \text{(E.5)}$$

The cation exchange reactions can be expressed with selectivity coefficients (Gaines and Thomas, 1953), that in the case of equation (E.5) will be:

$$^{M}_{Ca}K_{sel} = \frac{(N_M)^2(a_{Ca})}{(N_{Ca})(a_{Ca})^2} \quad \text{(E.5a)}$$

where a_M and a_{Ca} are the activities of the monovalent cations M and Ca; and N_M y N_{Ca} are the equivalent fractional occupancies.

The parameters defining the surface properties of C–S–H, including the site density, that will be used for the modelling are summarised in Table 2.

Missana et al. (2017) showed that the presence of alkali ions (M^+ = Na, K and Cs) decreased Ba adsorption on C–S–H (0.8) and simulated the curves of the K_d variation for Ba in the presence of increasing quantities of alkalis with the SWE model and indirectly determined the constants for surface complexation and ion exchange for Cs and Na in the CSH (0.8).

Therefore, the validity of this model for Cs and Na sorption data in a wider range of experimental conditions will be verified first. Then, the possibility of describing the experimental data with simpler models will be discussed. Different models will be tested trying to reproduce the adsorption behaviour in the different C–S–H phases and their surface charge upon adsorption. The data of competence of Na and Cs for Ba sorption will be considered as further constraint for modelling.

Model calculations were done with the CHESS code v 2.4 (van der Lee and De Windt, 1999) and the fits of the experimental curves were obtained with a step-wise trial and error procedure.

Table 2
Reactions and surface parameters used for sorption modelling. From Missana et al. (2017).

Description	Reaction	LogK	Site Density
Silanol (strong site, S)	$Si_sOH \Leftrightarrow Si_sO^- + H^+$	6.80 ± 0.5	$3.5{\cdot}10^{-3}$ μmol m^{-2}
Silanol (weak site, W)	$SiOH \Leftrightarrow SiO^- + H^+$	6.80 ± 0.5	13 μmol m^{-2}
Exchange site (E)	X_2Ca		2 μmol m^{-2}
Complexation of Ca (CSH charge)	$SiO^- + Ca^{2+} \Leftrightarrow SiOCa^+$	−4.12	

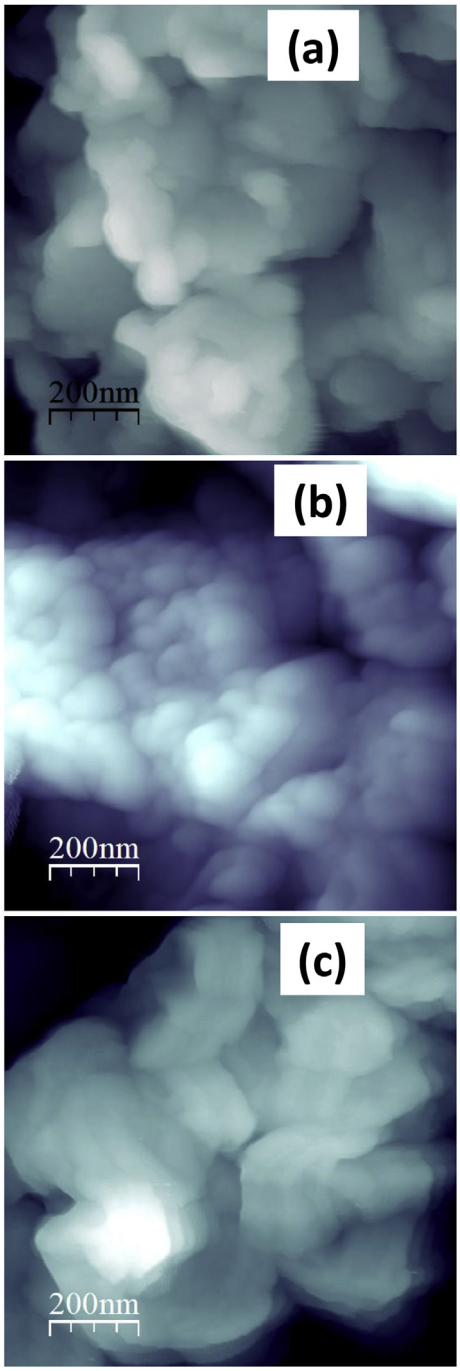

Fig. 1. AFM images of the C–S–H phases used in this study. a) Ca/Si = 0.8; b) Ca/Si = 1.2 and c) Ca/Si = 1.6.

3. Results and discussion

The morphology of the C–S–H upon their synthesis was analysed by AFM. Fig. 1 shows the AFM images of three different phases used in this study: C–S–H (0.8), C–S–H (1.2) and C–S–H (1.6) in Fig. 1a, b and 1c, respectively. The microstructure of the C–S–H gels is similar for all the phases with Ca/Si < 1.2, where large aggregated of particles in the nanometre range (50–200) are seen. The structure of the C–S–H (1.6) phase (Fig. 1c) is different, as more ordered structure are observed, with the presence of thicker crystals. This agrees with the decrease of the BET surface area for this phase, and with the precipitation of Ca-bearing minerals, as indicated in Missana et al. (2017).

Fig. 2 shows the kinetic test carried out with Cs in C–S–H (1.2)

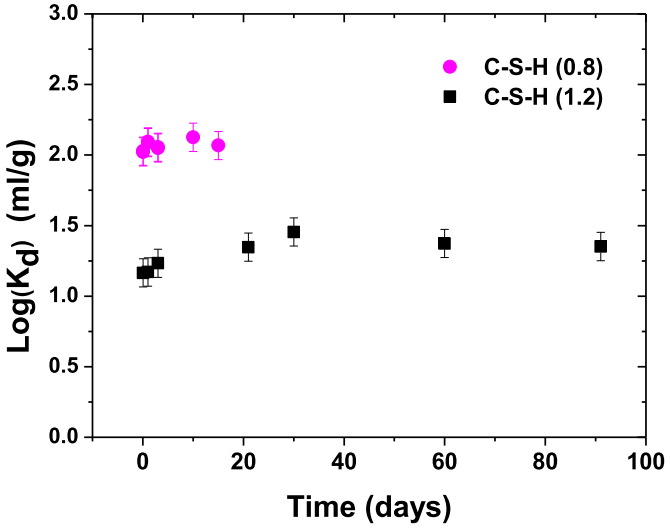

Fig. 2. Sorption of Cs as a function of time in (●) C–S–H (0.8) and (■) C–S–H (1.2). [Cs] = $1.3{\cdot}10^{-9}$ M.

(from 1 to 91 days) and C–S–H (0.8) (from 1 to 15 days). Results show that sorption of the RN is rapid and completed within few days, therefore for the sorption isotherms a contact time of 15 days was selected. Results obtained in the C–S–H (1.2) indicate that the sorption equilibrium is maintained over months, as the distribution coefficient does not vary with time, and that slower processes of incorporation or desorption are not occurring.

Additionally, the importance of Ca/Si ratio in Cs sorption is also deduced, as clearly sorption is higher for the lowest Ca/Si ratio.

The dependence of Cs and Na sorption on the Ca/Si ratio is better seen in the sorption isotherms shown in Fig. 3 for Cs (Fig. 3a) and Na (Fig. 3b). For both elements, the highest K_d values correspond to the C–S–H (0.8) phase, which has the lowest Ca/Si ratio; then K_d values decrease as the Ca/Si ratio increases, in agreement with previous studies.

Furthermore, from the experimental data in Fig. 3, it can be deduced that K_d values for Cs clearly vary with the radionuclide concentration, reflecting non-linear sorption, this effect being more evident at low Ca/Si ratios. Nevertheless, in the case of Na adsorption, the non-linearity is not clearly observed.

Quantitatively, sorption of Cs in C–S–H is appreciably higher than that of Na, only at trace concentration and at the lowest Ca/Si ratio, whereas at high tracer concentration K_d values are similar for both elements. In C–S–H (0.8), K_d values for Cs vary from approximately 170 to 15 mL g^{-1} and in the case of Na, K_d values range from approximately 35 to 25 mL g^{-1} and in the C–S–H (1.2), K_d values range from 25 to 8 mL g^{-1} for Cs and from 10 to 4 mL g^{-1} for Na.

For Cs, in the C–S–H (1) K_d values vary from approximately 80 to 10 mL g^{-1} and finally in C–S–H (1.6) sorption is quite low (< 5 mL g^{-1}) and experimental data (especially in log form) are more scattered.

In summary, sorption of Cs in the C–S–H is not very high (< 200 mL g^{-1}), and it is even less for Na (< 50 mL g^{-1}), however Na cannot be considered as indifferent ion towards C–S–H surface. The values reported here for Cs, agree with the data summarised by Ochs et al. (2016), which reported K_d values for Cs in C–S–H mainly from 1 to 600 mL g^{-1}.

For both elements, the dependence on the Ca/Si ratio is observed but only for Cs, sorption was clearly not linear. Thus, the main difference observed amongst the two elements in sorption tests, is their behaviour at trace concentrations. In this case, more selective sorption sites seem to exist for Cs, which must not be easily accessible for Na. For concentrations [M^+] > $1{\cdot}10^{-5}$ M, however, sorption is similar for both elements.

To aid the development of descriptive sorption models, the analysis of the electrophoretic properties of the gels before and after the alkalis uptake was performed. Fig. 4 shows the electrophoretic behaviour of C–S–H phases with different Ca/Si ratios, before and after the addition of Na or Cs. In particular, Fig. 4a shows the comparison of the ζ-potential values as a function of the Ca/Si ratio before and after the addition of a fixed quantity of Na or Cs ($3{\cdot}10^{-2}$ M) and Fig. 4b shows the variation of ζ-potential of the different C–S–H phases upon progressive addition of Na or Cs (from $2{\cdot}10^{-3}$ up to $5{\cdot}10^{-2}$ M).

As long reported in different studies (Viallis-Terrise et al., 2001; Nachbaur et al., 1998), the electrokinetic behaviour of the C–S–H phases as a function of the Ca/Si ratio (Fig. 4a), is consistent with the facts that Ca is the ion determining the potential (IDP), and that the surface charge is mainly determined by the balance of silanol deprotonation and Ca complexation with silanols (E.3 and E.4c). In the case of the phases used in this work, as already described by Missana et al. (2017), the point of zero charge is [Ca] = 3 mM, approximately. Thus, as can be seen in Fig. 4a, the phases with lower Ca/Si ratio (C–S–H (0.8) and C–S–H (1)), present negative surface charge while the other two exhibit positive charge. This observation, in addition to the fact that dissolved (potentially competing) Ca increases with the Ca/Si ratio (Table 1), can qualitatively explain the results of Fig. 3: i.e. that cations adsorption in C–S–H decreases as Ca/Si increases.

The differences in ζ-potential between the as-received and traced

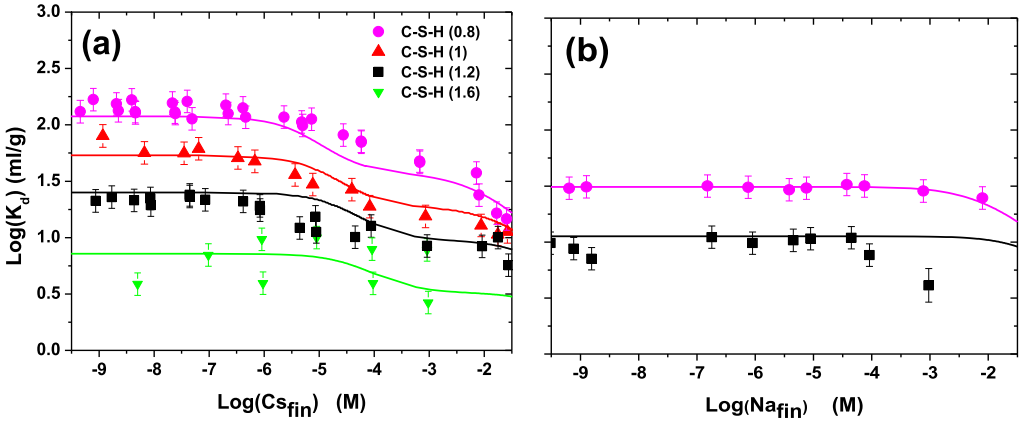

Fig. 3. Sorption isotherms of (a) Cs and (b) Na in: (●) C–S–H (0.8); (▲) C–S–H (1); (■) C–S–H (1.2) and (▼) C–S–H (1.6). Contact time 15 days. Solid lines correspond to the three-sites model (SWE) proposed by Missana et al. (2017).

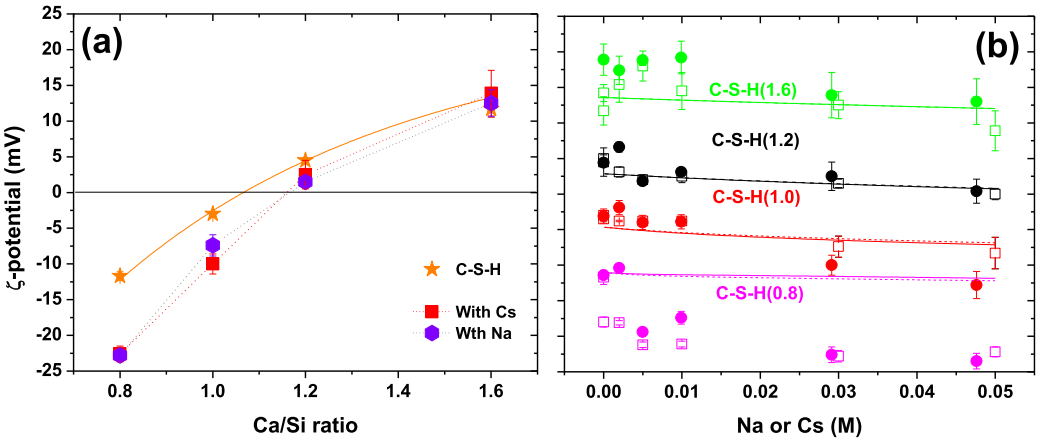

Fig. 4. (a) Comparison of the ζ-potential values as a function of the Ca/Si (★) before and after the addition of $3{\cdot}10^{-2}$ M of (⬢) Na or (■) Cs. (b) ζ-potential of the C−S−H phases (1 g/L) upon progressive addition of Na (open squares) or Cs (filled circles). In Figure 4b, solid/dotted lines correspond to the SWE model proposed by Missana et al. (2017) for Cs and Na, respectively.

C−S−H, are enhanced with the Ca/Si ratio, possibly according to larger alkali incorporation; it is maximum for C−S−H (0.8) (around 10 mV) and similar for Na and Cs. A small shift of the point of zero charge upon the alkalis ($3{\cdot}10^{-2}$ M) adsorption, towards higher Ca concentration (4.5 mM) is deducible from data of Fig. 4a, indicating that along with equilibriums with Ca, some specificity in retention process may exist. However, specific mechanisms of alkalis interaction or differences between Cs and Na cannot be derived in a straightforward way from electrokinetic data.

The same conclusion can be derived from Fig. 4b, which shows the progressive variation of the C−S−H ζ-potential, upon the addition of Ca/Na. In all the cases, a slight tendency of the ζ-potential to decrease, as the alkali ion is added, is observed but this variation is always small (< 5 mV) and only in the case of C−S−H (0.8) the variation is more evident. Within the experimental error, no differences between Cs and Na are seen. This is not surprising, considering that in the electrokinetic experiments the loading of the two elements is high ($> 10^{-4}$ M) and in this region of the isotherms, differences between Na and Cs sorption are barely seen.

The first step of the modelling phase consists on verifying if the surface model for C−S−H developed in Missana et al. (2017) and the constant indirectly determined for Na, Cs (and K) with the SWE model are valid; then the possibility of using simpler models will be evaluated. Table 3 and Table 4 summarises all the sorption parameter obtained analysing different models, for Na and Cs respectively.

The simulations obtained with the SWE model for Na and Cs sorption isotherm (Fig. 3) and the ζ-potential (Fig. 4b) data are superimposed to the experimental data.

As can be seen in both these figures, this SWE model is adequate to reproduce the adsorption and electrokinetic data of both Cs and Na under most of the experimental conditions, and the constants obtained by fit of data in Figs. 3 and 4b for the C−S−H (0.8) are the same as that proposed in Missana et al. (2017) (see Tables 3 and 4). The main flaw in the model is seen for the fit of the C−S−H (0.8) ζ-potential data, as the model clearly underestimate them.

If the parameters of the models for Cs and Na are compared, the contribution of the weak and exchange sites is very similar for Na and Cs, whereas the contribution of sorption in strong sites is much lower, and probably negligible, for Na. This is in agreement with the hypothesis, made after the analyses of the experimental data, that the main difference between Cs and Na sorption behaviour consists on the fact that strong sites are accessible for Cs and not for Na.

This finding agrees to that reported by Bach et al. (2013) who observed that K could be retained in the C−S−H *interlayers* but not Na, and also with the results of Chen and Brouwers (2010), who found that Na sorption was linear in contrast to K, which complied with the Freundlich isotherms. This indicates that amongst the alkalis, mayor similitude is observed between K and Cs than Na.

The surface complexation constants used to simulate C−S−H (0.8) sorption are slightly higher than those needed to simulate the other phases, but the standard deviation of the mean values is not very large with respect to the experimental error, possibly indicating similar sorption mechanisms for all Ca/Si ratio. However, it seems that the selectivity in silanol sites (especially strong ones) decreases when the Ca/Si ratio increases, in agreement with a lower reactivity, most probably due to the positive surface charge of C−S−H, which hampers solid/ions interactions.

The observation of Cs and (especially) Na experimental sorption

Table 3
Reactions and parameters used for different sorption models for Na in different C−S−H phases.

3-sites [SWE]					
Na	CSH (0.8)	CSH (1.0)	CSH (1.2)	CSH (1.6)	Mean
Complexation on strong sites (S)	−5.00		−5.30		−5.15 ± 0.21
Complexation on weak sites (W)	−5.50		−5.70		−5.60 ± 0.14
M^+ exchange (E)	0.37		0.37		0.37 ± 0.00
2-sites [WE]					
Complexation on weak sites (W)	−5.50		−5.70		−5.60 ± 0.10
M^+ exchange (E)	0.47		0.37		0.42 ± 0.05
2-sites [SW]					
Complexation on strong sites (S)	−4.80		−4.9		−4.85 ± 0.05
Complexation on weak sites (W)	−5.40		−5.60		−5.50 ± 0.10
2-sites [SE]					
Complexation on strong sites (S)	−5.60		−5.80		−5.70 ± 0.10
M^+ exchange (E)	0.82		0.74		0.78 ± 0.04
1-site [W]					
Complexation on weak sites (W)	−5.40		−5.65		−5.2 ± 0.13
1-site [E]					
M^+ exchange (E)	0.82		0.74		0.78 ± 0.04

Table 4
Reactions and parameters used for different sorption models for Cs in different C–S–H phases.

3-sites [SWE]					
Cs	CSH (0.8)	CSH (1.0)	CSH (1.2)	CSH (1.6)	Mean
Complexation on strong sites (S)	−1.75	−2.00	−2.20	−2.30	**−2.06 ± 0.24**
Complexation on weak sites (W)	−5.40	−5.60	−5.80	−5.80	**−5.65 ± 0.19**
M^+ exchange (E)	0.27	0.27	0.37	0.37	0.32 ± 0.06
2-sites [SW]					
Complexation on strong sites (S)	−1.75	−2.00	−2.20	−2.20	−2.04 ± 0.18
Complexation on weak sites (W)	−5.30	−5.60	−5.80	−5.80	−5.63 ± 0.20
2-sites [SE]					
Complexation on strong sites (S)	−1.75	−2.00	−2.20	−2.30	−2.06 ± 0.21
M^+ exchange (E)	0.87	0.77	0.67	0.65	0.74 ± 0.09

data and of the parameters obtained used with the SWE model, suggests that simpler models can be adopted for data description.

Thus, the second part of the modelling study consisted on the evaluation of possible simpler sorption models able to satisfactorily reproduce sorption and ζ-potential data for Cs and Na presented in this work. The parameters defining the C–S–H surface (sites and site density, Table 2) are not changed, but combination of possible reactions at these sites, will be evaluated. The data of competence of Na and Cs on Ba sorption (Missana et al. (2017) will be used as additional constraint to verify the model parameters validity.

Sodium data will be initially analysed. Considering that Na sorption is linear (Fig. 3b) one-site models will be evaluated first. Considering the small density of strong silanol sites, they will be saturated a relatively low tracer concentration ($1{\cdot}10^{-6}$-$1{\cdot}10^{-5}$ M), behaviour not seen in the experimental Na data, thus sorption exclusively on strong silanol sites (S) is not a possible option and it was discarded. Therefore, the two other possible options are: a) sorption in weak silanol sites (W) or b) sorption in exchange sites (E). In the case of two-sites models, three possibilities will be evaluated for Na: a) complexation in strong and weal silanol sites (SW); b) complexation in strong silanol sites and exchange sites (SE); c) complexation in weak silanol sites and exchange sites (WE).

Fig. 5 shows the comparison of the simulations obtained for the Na data, with the different models. In the Figure, the first row corresponds to one-site models (W and E) and the second row to two-sites models (SW, SE and WE).

Fig. 5a shows the fits of Na sorption isotherms data; Fig. 5b the fit of ζ-potential data upon Na adsorption and Fig. 5c the fit of the sorption curves of Ba in presence of Na, presented in Missana et al. (2017). The parameters used for these fits are summarised in Table 3.

In general, it can be observed that equivalent simulations for both sorption isotherms and ζ-potential data can be obtained in all the cases, being the main drawback of the simulation of the evolution of ζ-potential of C–S–H (0.8), as already observed with the SWE model.

These simulations of Na sorption and ζ-potential data (Fig. 5a, b and 5c) with one or two-sites models are also comparable to that obtained with the three-sites model previously described.

For one-site models, the parameter determination is straight from the isotherm data (with the uncertainty derived by the experimental error). Within this variation, all the data can be satisfactorily simulated, even if it appears that the simulations in Fig. 5c, tend to slightly underestimate the Na competence effects on Ba adsorption (a plateau is

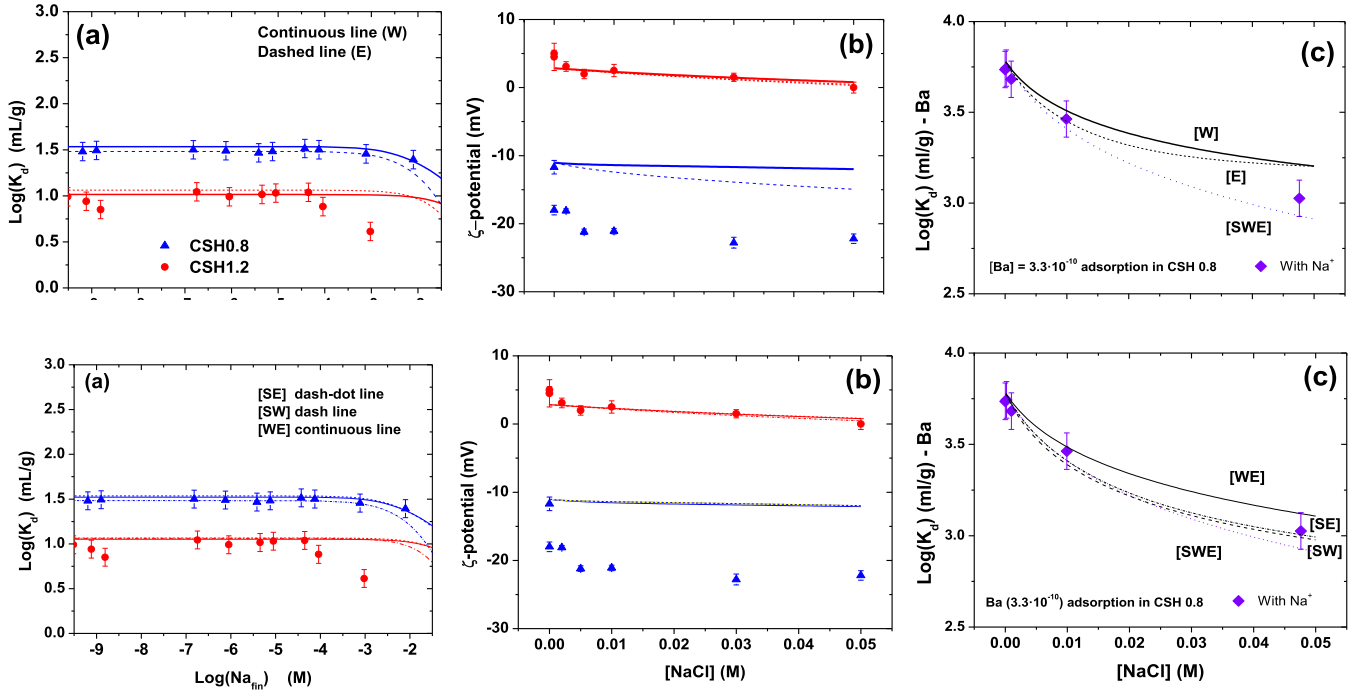

Fig. 5. Comparison of different models for Na uptake on C–S–H. First raw: one-site models; second raw: two-sites models. (a) Fit of Na sorption isotherms; (b) fit of ζ-potential data upon Na adsorption and c) fit of the sorption curves of Ba in presence of Na.

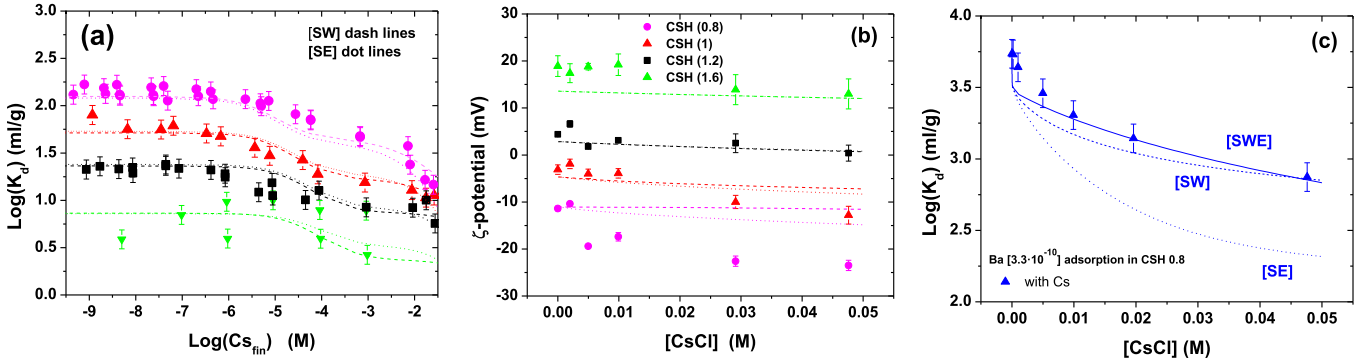

Fig. 6. Comparison of different models for Cs uptake on C–S–H. (a) Fit of Cs sorption isotherms; (b) fit of ζ-potential data upon Cs adsorption and c) fit of the sorption curves of Ba in presence of Cs. (●) C–S–H (0.8); (▲) C–S–H (1); (■) C–S–H (1.2) and (▼) C–S–H (1.6).

reached).

The addition of a second site helps to improve the fit of data in Fig. 5c because it causes a change in the initial slope of the competence curve. This is the case of SE or SW model; adding the (small) contribution of sorption in the strong silanol sites (imperceptible in the isotherms) the simulations of Fig. 5a slightly improve, in respect to E or W, one-site models. This can be an indication that, even if cannot be detected in the isotherms, this small contribution might be true.

The main problem observed evaluating two-sites models for Na, was related to the existence of several possible combinations of parameters fitting sorption data. Thus, the use of further independent experimental data (i.e. previous data of competence of Na and Cs on Ba sorption) was critical to constrain the model.

In the case of Cs, one-site models were discarded because, as it can be deduced directly from the isotherm data, that adsorption is non-linear, and therefore at least two sorption sites are necessary to fit sorption data. One-site models, cannot fit the isotherms in the entire range of Cs concentration investigated. Furthermore, to reproduce correctly the shape of the isotherms, one of the two sorption sites must have relatively low density. Therefore, the two unique possible options are: a) complexation in strong and weak silanol sites (SW) and b) complexation in strong silanol sites and exchange sites (SE).

Fig. 6 shows the comparison of the simulations obtained for the Cs data. Fig. 6a shows the fits of Cs sorption isotherms data; Fig. 6b the fit of ζ-potential data upon Cs adsorption and Fig. 6c the fit of the sorption curves of Ba in presence of Cs, presented in Missana et al. (2017). The parameters used for these fits are summarised in Table 4.

As can be seen in Fig. 6a and b the simulation of the data with SW and SE models are of similar quality, and equivalent to the three-sites (SWE) model, but data in Fig. 6c could not be similarly fit with the SE model.

From this modelling exercise, it seems that the simplest possible alternative model fit all the experimental data of Cs is the two-site model, which includes complexation reactions on weak and strong silanol sites (SW). This model could be satisfactorily used also for Na.

Again, comparing the modelling parameters obtained for the two-sites models of Na and Cs, it arises that the main difference corresponds to the strong silanols sites, which are highly selective for Cs but not for Na.

4. Conclusions

Sorption of Na and Cs on C–S–H gels was investigated by batch experiments, electrophoretic measurements and sorption modelling. The effect of Ca/Si ratio and of tracer concentration was evaluated as well as the similitudes/differences in the behaviour of both elements.

Alkalis sorption on C–S–H decreases as the Ca/Si ratio increases. Sorption of Cs is higher than that of Na, mainly at trace concentration and in the C–S–H phases with the lower Ca/Si ratio. This occurs because Cs sorption is not linear, thus basically, results show that in C–S–H strong sorption sites exists with low density and high selectivity for Cs which are (almost) not accessible for Na.

To simulate the experimental data (sorption isotherms, electrokinetic measurements and effects of presence of Na or Cs on Ba adsorption) different models were tested. The first option was the three-site model proposed by Missana et al. (2017), which fit satisfactorily the entire data set, but the electrokinetic data in C–S–H (0.8). These last mentioned data could not be reproduced by any of the tested models.

The analyses of data indicated that in the case of alkalis sorption a simplified modelling approach could be used. In the case of Na, it is possible to fit the data similarly well with one-site or two-sites models, even if two-sites models appear more adequate to simulate the competence effects played by Na on Ba adsorption.

In the case of Cs, due to the non-linearity of its sorption one-site models could not be used. Amongst the two-sites model, the one including surface complexation on weak and strong sites (SW) was shown to be the best to simulate the whole of experimental data.

Modelling data confirms that the main difference between Cs and Na sorption is mainly at a trace concentration ($< 10^{-5}$ M) due to the existence of sorption sites with low density but high selectivity for Cs, which are not accessible to Na.

The importance of using different independent experimental data to develop sorption models has been shown to be very important for these systems.

Acknowledgements

This work has been carried out under the frame of the MIRAME Project (CTM2014-60482-P) supported by the Spanish Ministry of Economy and Competitiveness.

References

Atkins, M., Glasser, F.P., 1992. Application of Portland cement-based materials to radioactive waste immobilization. Waste Manag. 12, 105–131.
Bach, T.T.H., Chabas, E., Pochard, I., Cau Dit Coumes, C., Haas, J., Frizon, F., Nonat, A., 2013. Retention of alkali ions by hydrated low-pH cements: mechanisms and Na^+/K^+ selectivity. Cement Concr. Res. 51, 14–21.
Chen, J.J., Thomas, J.J., Taylor, H.F.W., Jennings, H.M., 2004. Solubility and structure of calcium silicate hydrate. Cement Concr. Res. 74, 1499–1519.
Chen, Q.Y., Tyrer, M., Hills, C.D., Yang, X.M., Carey, P., 2009. Immobilisation of heavy metals in cement-based solidification/stabilization: a review. Waste Manag. 29, 390–403.
Chen, W., Brouwers, H.J.H., 2010. Alkali binding in hydrated Portland cement paste. Cement Concr. Res. 40 (5).
Delgado, A.V., González-Caballero, F., Hunter, R.J., Koopal, L.K., Lyklema, J., 2007. Measurements and interpretation of electrokinetic phenomena. J. Colloid Interface Sci. 309, 194–224.
Dzombak, D.A., Morel, F.M., 1990. Surface Complexation Modelling: Hydrous Ferric

Oxide. John Wiley and Sons.
Evans, N.D.M., 2008. Binding mechanisms of radionuclides to cements. Cement Concr. Res. 38 (4), 543–553.
Gaines, G.I., Thomas, H.C., 1953. Sorption studies on clay minerals II. A formulation of the thermodynamics of exchange sorption. J. Chem. Phys. 21, 714–718.
Heat, T.G., Ilett, D.J., Tweed, C.J., 1996. Thermodynamic modelling of the sorption of radioelements onto cementitious materials. Mater. Res. Soc. Symp. Proc. 412, 443–449.
Henocq, P., 2017. A sorption model for alkalis in cement-based materials – correlations with solubility and electrokinetic properties. Phys. Chem. Earth 99, 184–193.
Hong, S.Y., Glasser, F.P., 1999. Alkali binding in cement pastes. Part I. The C-S-H phase. Cement Concr. Res. 29, 1893–1903.
Horcas, I., Fernández, R., Gómez-Rodriguez, J.M., Colchero, J., Gómez-Herrero, J., Baro, A.M., 2007. WSXM: a software for scanning probe microscopy and a tool for nanotechnology. Rev. Sci. Instrum. 78, 013707.
Huang, C.P., Stumm, W., 1973. Specific adsorption of cations hydrous Al_2O_3. J. Colloid Interface Sci. 231–259.
Hunter, R.J., 1991. Zeta Potential in Colloid Science. Academic Press, pp. 398.
Hunter, R.J., 1992. Foundations of Colloid Science, vol. II Oxford Science Publications, Clarendon Press.
Iwaida, T., Nagasaki, S., Tanaka, S., Yaita, T., Tachimori, S., 2002. Structure alteration of C-S-H caused by sorption of caesium. Radiochim. Acta 90, 677–681.
Lothenbach, B., Nonat, A., 2015. Calcium silicate hydrates; solid and liquid phase composition. Cement Concr. Res. 78, 57–70.
Missana, T., García-Gutiérrez, M., Mingarro, M., Alonso, U., 2017. Analyses of barium reention mechanisms on calcium silicate hydrate phases. Cement Concr. Res. 93, 8–16.
Nachbaur, L., Nkinamubanzi, P.C., Nonat, A., Moutin, J.C., 1998. Electrokinetic properties which controls the coagulation of silicate cement suspensions during early stage hydration. J. Colloid Interface Sci. 202, 261.
Ochs, M., Mallants, D., Wang, L., 2016. Radionuclide and Metal Sorption on Cement and Concrete, Topics in Safety, Risk, Reliability and Quality. Springer, Switzerland.
Ochs, M., Pointeau, I., Giffaut, E., 2006. Caesium sorption by hydrated cement as a function of degradation state: experiments and modelling. Waste Manag. 26 (7), 725–732.
Pointeau, I., 2000. Etude mécanistique et modélisation de la retention de radionucléides par les phases de silicate de calcium des ciments hydrates. Thèse de l'Université de Reims-Champagne Ardennes, France.
Stade, H., 1989. On the reaction of C–S–H(di, poly) with alkali hydroxides. Cement Concr. Res. 19 (5), 802–810.
Sugiyama, D., 2008. Chemical alteration of C-S-H in sodium chloride solution. Cement Concr. Res. 38, 1270–1275.
Tits, J., Wieland, E., Müller, C.J., Bradbury, M.H., 2006. Strontium binding by calcium silicate hydrates. Journal of Colloids and interface Science 300 (1), 78–87.
Tits, J., Ijima, K., Wieland, E., Kamei, G., 2006b. The uptake of radium by calcium silicate hydrates and hardened cement paste. Radiochim. Acta 94, 637–643.
Van der Lee, J., de Windt, L., 1999. CHESS Tutorial and Cookbook. Technical Report LHM/RD/99/05.
Viallis, H., Faucon, P., Petit, J.C., Nonat, A., 1999. Interaction between salts (NaCl, CsCl) and C-S-H. J. Phys. Chem. B 103, 5212–5219.
Viallis-Terrisse, H., Nonat, A., Petit, J.C., 2001. Zeta-potential study of calcium silicate hydrates interacting with alkaline cations. J. Colloid Interface Sci. 244 (1), 58–65.
Viallis-Terrisse, H., Nonat, A., Petit, J.C., Landesman, C., Richet, C., 2002. Specific interaction of cesium with the surface of calcium silicate hydrates. Radiochim. Acta 90, 699–704.